ORIGINAL ARTICLE

Drying properties, color characteristics, microstructure, and modeling of ginger cubes dried using electrohydrodynamic, electrohydrodynamic-hot air, and hot air methods

Ahmet Polat[1] · Nazmi Izli[1]

Abstract

This study investigates the drying of ginger cubes using three different techniques: electrohydrodynamic drying, electrohydrodynamic-hot air drying, and hot air drying. The main objective is to assess how these drying methods affect drying times, effective diffusion coefficients, color, and microstructure. Additionally, the study includes fitting ten different thin-layer models to the experimental data for mathematical analysis. It was observed that increasing temperature and voltage values led to a reduction in the drying times of the ginger samples. After conducting statistical tests, it was determined that the Midilli et al. and Wang and Singh models were the most suitable for describing the experimental drying curves. Effective diffusion coefficient values increased with the rise in temperature and voltage values. The L^* values of the dried ginger samples decreased due to temperature and voltage applications. Notably, ginger samples dried using the electrohydrodynamic method exhibited better preservation of their original appearance, particularly in terms of microstructure and starch particle integrity, compared to other drying methods. The findings of the study suggest that integrating electrohydrodynamic technology with hot air drying reduces overall drying time. This innovative approach shows promise for producing high-quality end products in the future.

1 Introduction

Ginger (*Zingiber officinale* Roscoe) is a monocotyledonous plant native to Southeast Asia and a member of the Zingiberaceae family [1]. It is not only utilized as a flavoring or fragrance in cuisine but also possesses health-promoting properties due to its abundance in bioactive components such as carotene, flavonoids, phenolics, and vitamins [2]. Ginger exhibits anti-inflammatory and antioxidative activities, acts as various anti-platelet and antitumor activators, and demonstrates anti-nausea and vomiting activity related to pregnancy, among its health-promoting functions [3]. Ginger with a high moisture content (ranging from 85 to 95%) is susceptible to microbial spoilage and chemical

degradation. Through the process of drying, the moisture content in the product is reduced, preventing reactions that cause microbial growth and degradation. Consequently, dried ginger, with a long storage period and suitability for consumption out of season, is obtained [4]. Dried ginger finds applications as a spice and as an auxiliary ingredient in the production of candies, soft drinks, pharmaceuticals, and cosmetics. However, the chosen drying method can lead to undesired alterations in the physical and chemical sensory characteristics of the product. Therefore, new drying technologies focus on achieving better quality products, lower costs, and more environmentally friendly features [5]. Developed as a novel technology, the electrohydrodynamic (EHD) drying method has significant potential for temperature-sensitive products due to its non-thermal feature [6]. The EHD drying system relies on the generation of a secondary airflow known as the ionic or corona wind. This airflow is produced by applying a high voltage to a curved electrode, typically in the form of a needle or wire. At elevated electrical voltages, the air surrounding the sharp electrode undergoes ionization, resulting in the generation of ions possessing the same polarity as the sharp electrode. These ions are propelled toward the grounded electrode

✉ Ahmet Polat
ahmetpolat@uludag.edu.tr

Nazmi Izli
nazmiizli@gmail.com

1 Department of Biosystems Engineering, Faculty of Agriculture, Bursa Uludag University, Gorukle Campus, 16059 Bursa, Turkey

at high velocities. As these ions move, they transfer their momentum to neutral air molecules through collisions. This abundant formation of ions, migrating towards the grounded electrode, is commonly referred to as the "corona wind". The presence of the corona wind induces instability in the boundary layer between the surrounding air and the product's surface. Consequently, both heat and mass transfer coefficients experience an increase, accelerating the rate of moisture removal [7]. Research involving EHD indicates that the corona wind exhibits its greatest effectiveness during the initial stages of the drying process, with diminishing effectiveness as drying progresses. To enhance the drying rate and facilitate moisture transport to the surface, researchers are considering the incorporation of an auxiliary heating method into the system. In the literature, studies exist where convective and EHD drying methods are used in combination [8, 9].

The objective of this research was to assess the drying times, effective diffusivity coefficient, color variations, and microstructural characteristics of ginger samples subjected to drying methods involving electrohydrodynamic (EHD), hot air, and the combined EHD-hot air technique. Additionally, the moisture content data obtained through experimental drying of ginger samples under varying conditions were compared to ten distinct thin-layer drying models utilized in this investigation, with the identification of the most suitable model for explaining the experimental findings.

2 Materials and methods

2.1 Sample preparation

Samples of Chinese-origin ginger (*Zingiber officinale*) were obtained from a local market and stored in a cooler maintained at a consistent temperature of 4 ± 0.01 °C until the initiation of the drying experiments. Prior to drying, the ginger products were retrieved from the cooler and allowed to reach room temperature. These ginger samples, showing no signs of

microbial degradation or physical damage, were then peeled and sliced to achieve an average thickness of 4.51 ± 0.57 mm. The sliced ginger samples were further cubed to dimensions of 11.83 ± 0.15 mm and 11.3 ± 0.75 mm. For each experiment, a precisely measured 100 ± 0.01 g sample was used. The initial moisture content of the product was determined to be 8.98 (dry basis) by subjecting the samples to a 24-h drying period.

2.2 Experimental procedure

In the Electrohydrodynamic (EHD) system, six wires with a diameter of 0.4 mm are positioned at intervals of 50 mm. In this research, the ginger product underwent drying through three different methods: EHD, hot air, and a combination of EHD with hot air. Two distinct voltage settings (20 and 30 kV) and two temperature settings (50 and 55 °C) were employed for the drying processes. These drying processes were conducted within controlled laboratory conditions, with a temperature of 26.8 °C and humidity at 28.3%, all while maintaining a constant air velocity of 1.5 m/s for each application. A separation distance of 30 mm was maintained between the EHD system and the ginger product. The moisture content alterations of the product during drying were monitored using precise scales positioned beneath the oven. The experiments were carried out in triplicate to ensure accuracy and consistency.

2.3 Thin-layer modeling

The thin-layer drying models used to characterize the drying profiles resulting from the experimental conditions applied to ginger samples dried using various methods are presented in Table 1. The dimensionless moisture ratio (MR) value, an essential parameter in these formulas, was calculated using Eq. (1) [20]:

$$MR = \frac{M_t - M_e}{M_o - M_e} \tag{1}$$

In this context, the variables M_e, M_t, and M_o represent the following parameters: M_e stands for the equilibrium moisture

Table 1 Thin layer mathematical modeling equations to be used for the comparison of the moisture ratio values

No	Model name	Model	References
1	Henderson and Pabis	$MR = a\exp(-kt)$	[10]
2	Newton	$MR = \exp(-kt)$	[11]
3	Page	$MR = \exp(-kt^n)$	[12]
4	Logarithmic	$MR = a\exp(-kt) + c$	[13]
5	Two term	$MR = a\exp(-k_0 t) + b\exp(-k_1 t)$	[14]
6	Two term exponential	$MR = a\exp(-kt) + (1-a)\exp(-kat)$	[15]
7	Wang and Singh	$MR = 1 + at + bt^2$	[16]
8	Diffusion Approach	$MR = a\exp(-kt) + (1-a)\exp(-kbt)$	[17]
9	Verma et al	$MR = a\exp(-kt) + (1-a)\exp(-gt)$	[18]
10	Midilli et al	$MR = a\exp(-kt^n) + bt$	[19]

content (expressed in kg of water per kg of dry matter), M_t represents the initial moisture content, and M_o signifies the moisture content at any given time during the process. Since M_e value in the formula is immeasurably small compared to other values, Eq. (2) is used instead of Eq. (1) in some studies [21]:

$$MR = \frac{M_t}{M_o} \tag{2}$$

2.4 Determination of effective diffusion coefficient

Equation (3) is one of the simplifications of Fick's second law of moisture diffusion given by Crank [22], was used to determine the effective diffusion coefficient of drying.

$$MR = \frac{8}{\pi^2} \sum_{n=0}^{\infty} \frac{1}{(2n+1)} \exp\left[-(2n+1)^2 \frac{\Pi^2 D_{eff} t_i}{4L^2}\right] \tag{3}$$

where D_{eff} is the effective diffusion coefficient (m²/s) and L is the half thickness of the ginger cubes. Equation (3) can be simplified to a one-term exponential model to determine the effective diffusion coefficient for drying food samples in logarithmic form as in Eq. (4) [23]:

$$\ln(MR) = \ln\frac{8}{\pi^2} - \frac{\Pi^2 D_{eff} t_i}{4L^2} \tag{4}$$

The effective diffusion coefficient was obtained by plotting $\ln(MR)$ versus drying time, t_i. The slope of the plot is shown in Eq. (5):

$$Slope = \frac{\Pi^2 D_{eff}}{4L^2} \tag{5}$$

2.5 Determination of color measurement

CIE Lab color parameters, namely $L*$, $a*$, and $b*$, were utilized to assess the surface color changes in both fresh and dried ginger samples. The $L*$ parameter, with a value of 0 signifying black and 100 representing white, reflects lightness. On the other hand, the $a*$ and $b*$ values span the red-green spectrum from +60 (indicating red) to -60 (indicating green) and the yellow-blue spectrum from +60 (indicating yellow) to -60 (indicating blue), respectively [24]. Before obtaining color measurements from the products, a colorimeter (MSEZ-4500 L, HunterLab, USA) was calibrated using standard black and white plates. Color readings were collected from five different points on the product's surface. The ΔE value, indicating the overall color change from fresh ginger samples to dried ones, along with Chroma (C), which signifies color intensity,

and Hue angle ($\alpha°$) values (0° representing pure red color, 90° representing pure yellow color, 180° representing pure green color, and 270° representing pure blue color), were determined using the following formulas. In these formulas, $L*$, $a*$, and $b*$ denote the color values of dried ginger samples, while L_0*, a_0*, and b_0* represent the color values of fresh ginger samples [25].

$$C = \sqrt{(a^2 + b^2)} \tag{6}$$

$$\alpha = \tan^{-1}\left(\frac{b}{a}\right) \tag{7}$$

$$\Delta E = \sqrt{(L* - L_0*)^2 + (a* - a_0*)^2 + (b* - b_0*)^2} \tag{8}$$

2.6 Microstructure analysis

The impact of the drying processes on the structural alterations of the ginger product was investigated using a scanning electron microscope (SEM) device (EVO 40, Germany). The procedure involved cutting cross-sections from the same area of the products using a scalpel. These sections were then affixed to a double-sided adhesive sample holder. Subsequently, the product samples were coated with a gold–palladium mixture (60/40) under low-pressure conditions. Finally, the samples were introduced into the SEM device for a detailed examination of their microstructures [26]. Numerical analysis of the images obtained from the scanning electron microscope was conducted using ImageJ software [27].

2.7 Statistical analysis

Data entry and analysis, excluding modeling, were carried out using the Excel 2016 program. The JMP package program (Version 7.0, USA) was employed for data analysis. In modeling studies, MATLAB (MathWorks Inc., Natick, MA) was employed. The suitability of the selected model was assessed by comparing the modeled moisture ratio values with the experimental data. To determine the most suitable model for explaining the drying behavior of the ginger product, statistical parameters such as the coefficient of determination (R^2), chi-square (χ^2), and root mean square error ($RMSE$) were employed. The calculations for chi-square (χ^2) and root mean square error ($RMSE$) were performed using the following formulas [28]:

$$RMSE = \sqrt{\frac{\sum_{i=1}^{n} (MR_{pre,i} - MR_{exp,i})^2}{N}} \tag{9}$$

$$\chi^2 = \frac{\sum\limits_{i=1}^{N}(MR_{\exp,i} - MR_{pre,i})^2}{N - z} \qquad (10)$$

In the formula, "$MR_{pre,i}$" and "$MR_{\exp,i}$" are denoted as the estimated moisture ratio for test number i, and the corresponding experimental moisture ratio for test number i, respectively. Additionally, "N" represents the count of observed experimental data, while "z" signifies the number of independent variables within the model.

3 Results and discussion

3.1 Drying times of ginger cubes

Figure 1 illustrates the drying curves of ginger samples subjected to various drying methods, including EHD at 20 and 30 kV, hot air at 50 and 55 °C, and EHD-hot air combinations (20 kV-50 °C, 20 kV-55 °C, 30 kV-50 °C, and 30 kV-55 °C). Initially, a notable weight loss rate is observed at the onset of the drying process, but this rate gradually diminishes as moisture content decreases and drying time extends [10]. Drying times across all drying

applications ranged from 120 to 480 min. Significantly, the EHD-combination method exhibited the shortest drying times. This observation aligns with the findings of Li et al. [29], who reported shorter drying times for okara cake samples subjected to the EHD-combination method (20 kV-105 °C) compared to control samples dried at 105 °C, consistent with our research. Specifically, drying times were recorded as 160, 140, 140, and 120 min for the 20 kV-50 °C, 20 kV-55 °C, 30 kV-50 °C, and 30 kV-55 °C drying applications, respectively. Elevating the temperature of products dried at the same voltage levels led to reduced drying times, while increasing the voltage levels for samples dried at the same temperature had a similar effect. A shift from 20 to 30 kV reduced the overall drying time by 12.5%, while an increase in temperature from 50 to 55 °C resulted in a 14.71% reduction in drying time. These findings underscore the role of electric field strength and temperature in shortening the drying process. Taghian Dinani et al. [30] observed a similar trend with voltage in a study on mushroom drying, and Sadeghi et al. [31] reported temperature-dependent reductions in drying time when studying lemon slice drying. These outcomes align with our study's results, highlighting the impact of voltage and temperature on drying efficiency.
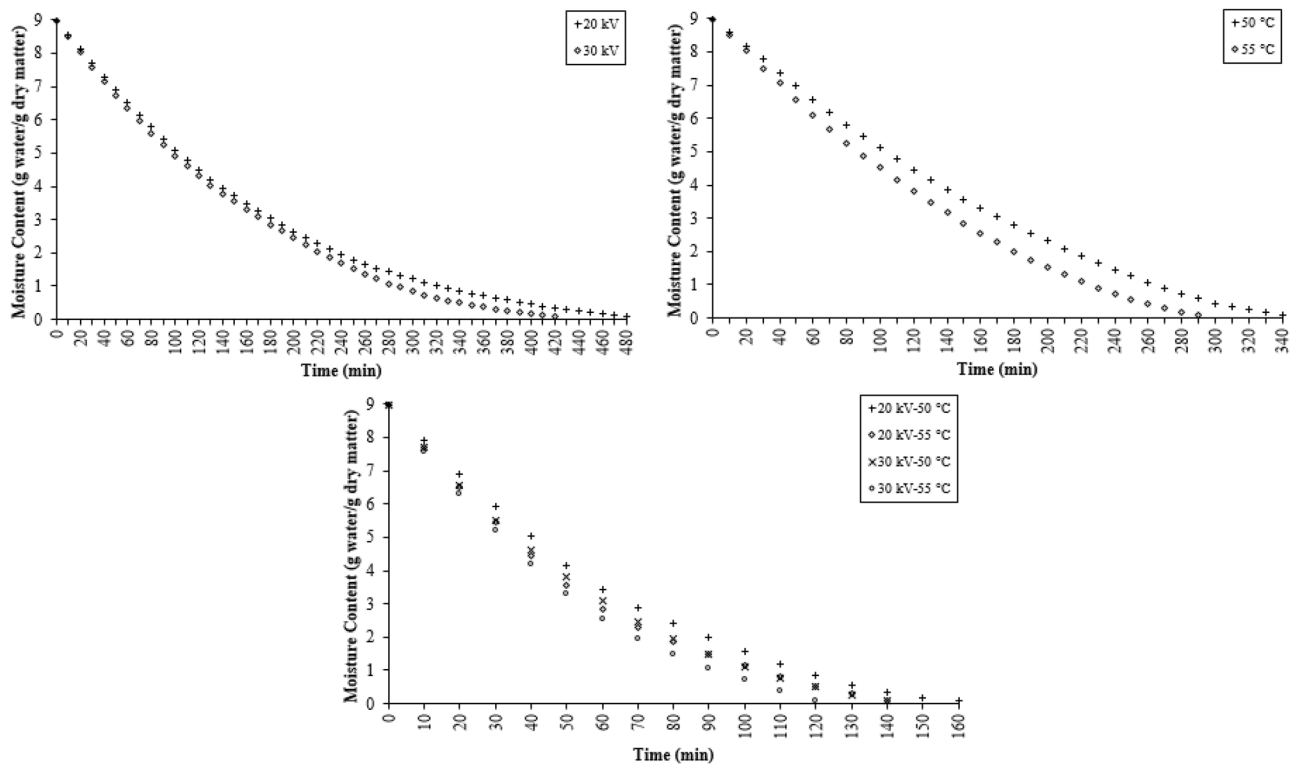

Fig. 1 The moisture content of ginger cubes dried with different methods over time

Table 2 Statistical analysis results on modeling of ginger cubes dried by EHD and hot air method

No	20 kV Model Katsayıları	R^2	RMSE	$\chi^2(10^{-4})$	30 kV Model Katsayıları	R^2	RMSE	$\chi^2(10^{-4})$	50 °C Model Katsayıları	R^2	RMSE	$\chi^2(10^{-4})$	55 °C Model Katsayıları	R^2	RMSE	$\chi^2(10^{-4})$
1	a=1.049 k=0.006546	0.9944	0.0216	4.6728	a=1.055 k=0.007076	0.9893	0.0304	9.2678	a=1.084 k=0.007289	0.9758	0.0475	22.5760	a=1.078 k=0.008585	0.9774	0.0460	21.1614
2	k=0.006241	0.9918	0.0262	6.8592	k=0.006714	0.9861	0.0347	12.0500	k=0.006713	0.9675	0.0551	30.3028	k=0.007949	0.9702	0.0528	27.9036
3	k=0.002691 n=1.16	0.9990	0.0093	0.8564	k=0.002374 n=1.201	0.9968	0.0167	2.7848	k=0.001157 n=1.345	0.9942	0.0233	5.4505	k=0.001573 n=1.328	0.9945	0.0226	5.1153
4	a=1.097 k=0.005359 c=-0.07983	0.9996	0.0057	0.3216	a=1.144 k=0.005221 c=-0.1337	0.9994	0.0071	0.5012	a=1.397 k=0.003889 c=-0.3813	0.9995	0.0067	0.4524	a=1.363 k=0.004761 c=-0.3482	0.9995	0.0069	0.4788
5	a=0.4137 k_0=0.006573 b=0.6346 k_1=0.006515	0.9942	0.0221	4.8821	a=0.5277 k_0=0.007075 b=0.5277 k_1=0.007087	0.9888	0.0312	9.7434	a=0.5414 k_0=0.007286 b=0.5414 k_1=0.007278	0.9742	0.0490	24.0336	a=0.8982 k_0=0.008547 b=0.1761 k_1=0 0.008582	0.9757	0.0478	22.8107
6	a=1.68 k=0.008169	0.9990	0.0091	0.8204	a=1.725 k=0.009009	0.9966	0.0172	2.9488	a=1.863 k=0.009819	0.9921	0.0272	7.4079	a=1.849 k=0.01153	0.9927	0.0261	6.8052
7	a=-0.004595 b=0.000005476	0.9954	0.0196	3.8380	a=-0.004942 b=0.0000063	0.9981	0.0130	1.6907	a=-0.004857 b=0.000005675	0.9999	0.0031	0.0947	a=-0.005785 b=0.000008173	0.9999	0.0025	0.0609
8	a=3.556 k=0.005016 b=0.9201	0.9947	0.0210	4.4211	a=0.77 k=0.006714 b=0.9996	0.9855	0.0356	12.6525	a=5.365 k=0.002426 b=0.7449	0.9994	0.0074	0.5468	a=5.08 k=0.003018 b=0.7463	0.9994	0.0073	0.5270
9	a=-5.075 k=0.003313 g=0.003675	0.9996	0.0055	0.3009	a=-2.405 k=0.002836 g=0.003665	0.9996	0.0073	0.5341	a=-2.774 k=0.001644 g=0.002567	0.9994	0.0074	0.5534	a=-2.635 k=0.00206 g=0.003184	0.9994	0.0073	0.5329
10	a=0.9952 k=0.00341 n=1.103 b=-0.00007317	0.9999	0.0017	0.0273	a=0.9918 k=0.003567 n=1.099 b=-0.0001574	0.9996	0.0061	0.3719	a=0.9953 k=0.002566 n=1.14 b=-0.000414	0.9997	0.0053	0.1841	a=0.9953 k=0.003253 n=1.134 b=-0.0004547	0.9997	0.0056	0.2299

Table 3 Statistical analysis results on modeling of ginger cubes dried by EHD-hot air combined method

| No	20 kV-50 °C				20 kV-55 °C				30 kV-50 °C				30 kV-55 °C			
	Model Katsayıları	R^2	RMSE	$\chi^2(10^{-4})$	Model Katsayıları	R^2	RMSE	$\chi^2(10^{-4})$	Model Katsayıları	R^2	RMSE	$\chi^2(10^{-4})$	Model Katsayıları	R^2	RMSE	$\chi^2(10^{-4})$
1	$a=1.056$ $k=0.01765$	0.9867	0.0365	13.3236	$a=1.045$ $k=0.02013$	0.9911	0.0296	8.8517	$a=1.046$ $k=0.01957$	0.9878	0.0350	23.7966	$a=1.046$ $k=0.02203$	0.9872	0.0364	13.2310
2	$k=0.01672$	0.9835	0.0407	16.5502	$k=0.01928$	0.9891	0.0330	10.8643	$k=0.01872$	0.9858	0.0377	14.2178	$k=0.02107$	0.9853	0.0390	15.2007
3	$k=0.005852$ $n=1.247$	0.9974	0.0163	2.6604	$k=0.008557$ $n=1.198$	0.9984	0.0128	1.6410	$k=0.007485$ $n=1.222$	0.9971	0.0170	2.8982	$k=0.00831$ $n=1.233$	0.9973	0.0166	2.7709
4	$a=1.18$ $k=0.01253$ $c=-0.1629$	0.9991	0.0096	0.9213	$a=1.135$ $k=0.01541$ $c=-0.1213$	0.9991	0.0093	0.8710	$a=1.174$ $k=0.01388$ $c=-0.1652$	0.9997	0.0054	0.2898	$a=1.189$ $k=0.01536$ $c=-0.1795$	0.9996	0.0067	0.4531
5	$a=2.73$ $k_0=0.009287$ $b=-1.716$ $k_1=0.006379$	0.9993	0.0086	0.7411	$a=1.892$ $k_0=0.01239$ $b=-0.8801$ $k_1=0.007208$	0.9992	0.0090	0.8018	$a=2.11$ $k_0=0.01085$ $b=-1.103$ $k_1=0.006311$	0.9997	0.0059	0.2913	$a=1.989$ $k_0=0.01223$ $b=-0.9813$ $k_1=0.006551$	0.9997	0.0060	0.3578
6	$a=1.785$ $k=0.02323$	0.9968	0.0179	3.2133	$a=1.733$ $k=0.02606$	0.9982	0.0133	1.7714	$a=1.751$ $k=0.02555$	0.9968	0.0180	3.2441	$a=1.766$ $k=0.02904$	0.9969	0.0178	3.1817
7	$a=-0.0123$ $b=0.0000388$	0.9987	0.0115	1.3268	$a=-0.01433$ $b=0.00005343$	0.9969	0.0175	3.0514	$a=-0.01384$ $b=0.00004938$	0.9987	0.0113	1.2769	$a=-0.01563$ $b=0.00006303$	0.9987	0.0115	1.3198
8	$a=4.844$ $k=0.008257$ $b=0.8233$	0.9991	0.0097	0.9310	$a=3.576$ $k=0.01076$ $b=0.792$	0.9991	0.0095	0.9018	$a=4.257$ $k=0.009499$ $b=0.8021$	0.9998	0.0042	0.1752	$a=3.991$ $k=0.01052$ $b=0.7788$	0.9996	0.0063	0.3939
9	$a=9.872$ $k=0.0281$ $g=0.03021$	0.9972	0.0169	2.8651	$a=7.894$ $k=0.03091$ $g=0.03357$	0.9984	0.0128	1.6311	$a=9.126$ $k=0.03067$ $g=0.03302$	0.9971	0.0171	2.9262	$a=9.937$ $k=0.03506$ $g=0.03757$	0.9972	0.0170	2.9151
10	$a=0.9991$ $k=0.008654$ $n=1.128$ $b=-0.0004192$	0.9997	0.0057	0.3285	$a=1.001$ $k=0.01147$ $n=1.106$ $b=-0.0003593$	0.9996	0.0060	0.3640	$a=0.9978$ $k=0.01125$ $n=1.091$ $b=-0.000554$	0.9999	0.0024	0.0615	$a=0.9991$ $k=0.0124$ $n=1.098$ $b=-0.0006527$	0.9999	0.0032	0.1055
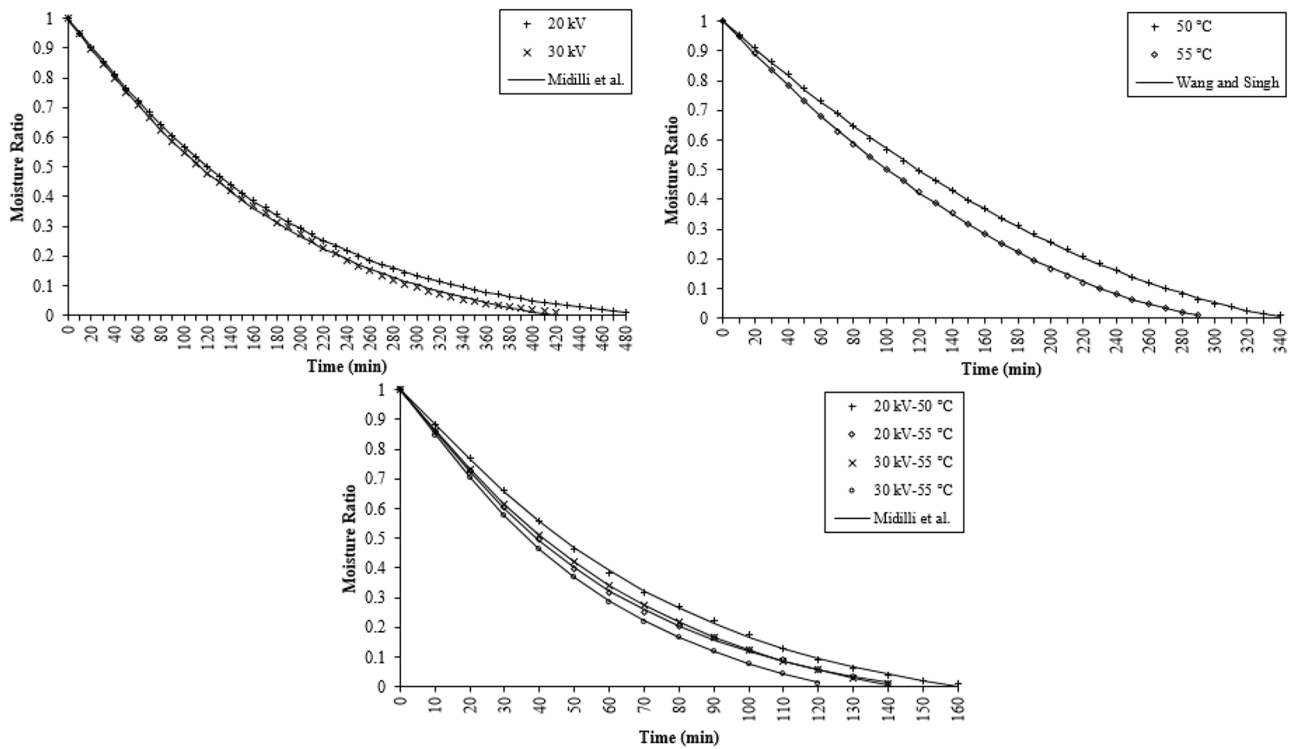
Fig. 2 Comparison of the experimental moisture ratios of ginger cubes dried under different conditions and the most selected models

3.2 Modeling of drying curves

In this study, EHD, hot air, and EHD-hot air combined methods were employed for drying thin layers of ginger cubes. The moisture ratio at different drying times was compared using ten different models: Henderson and Pabis, Page, Newton, Two-term, Logarithmic, Wang and Singh, Two-term exponential, Midilli et al., Verma et al., and Diffusion approximation. To determine the most suitable model, statistical parameters including the coefficient of determination (R^2), root mean square error (*RMSE*), and chi-square (χ^2) were utilized. Tables 2 and 3 present the constants and coefficients of the models obtained through multiple regression analysis. Upon examining the tables, it becomes evident

Table 4 Color values of fresh and dried ginger cubes with different drying methods

Drying Conditions	Color Parameters					
	L*	a*	b*	C	α°	ΔE
Fresh	74.984 (0.321)[a]	-3.244 (0.027)[f]	40.478 (0.089)[a]	40.608 (0.087)[a]	94.539 (0.046)[a]	-
EHD						
20 kV	63.630 (0.066)[c]	2.562 (0.062)[d]	28.170 (0.043)[g]	28.286 (0.040)[g]	84.846 (0.130)[d]	17.723 (0.504)[d]
30 kV	61.556 (0.193)[e]	3.902 (0.018)[a]	31.220 (0.119)[e]	31.463 (0.117)[e]	82.917 (0.047)[f]	17.807 (0.234)[d]
Hot Air						
50 °C	61.588 (0.208)[e]	2.896 (0.030)[c]	34.520 (0.100)[b]	34.641 (0.272)[b]	85.248 (0.471)[c]	15.895 (0.275)[b]
55 °C	59.922 (0.122)[f]	1.436 (0.022)[e]	29.774 (0.065)[f]	29.809 (0.867)[f]	87.283 (0.501)[b]	19.062 (0.483)[e]
EHD-Hot Air						
20 kV-50 °C	64.398 (0.226)[b]	2.812 (0.300)[c]	33.650 (0.248)[c]	33.768 (0.081)[c]	85.269 (0.053)[c]	13.982 (0.121)[a]
20 kV-55 °C	63.444 (0.061)[c]	3.528 (0.016)[b]	28.452 (0.084)[g]	28.670 (0.073)[g]	82.973 (0.029)[f]	17.991 (0.303)[d]
30 kV-50 °C	63.694 (0.609)[c]	3.460 (0.196)[b]	31.838 (0.891)[d]	32.026 (0.102)[d]	83.830 (0.039)[e]	15.723 (1.199)[b]
30 kV-55 °C	62.080 (0.144)[d]	2.794 (0.011)[c]	31.186 (0.074)[e]	31.311 (0.066)[e]	84.923 (0.038)[d]	17.009 (0.135)[c]

The statistics of each color parameter column have been applied separately, and the differences between the means with different letters in the same column are significant ($p < 0.05$)
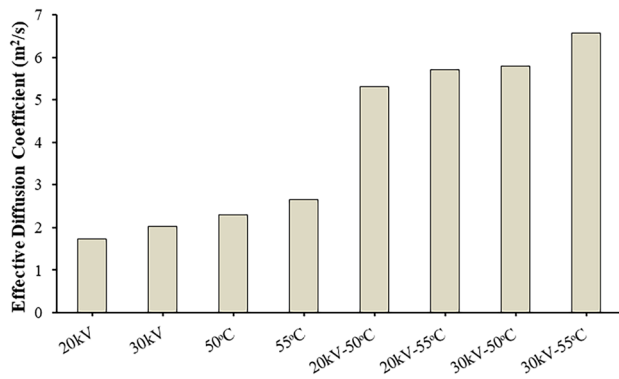
Fig. 3 Effective diffusion coefficient values of dried ginger cubes with different drying methods

Fig. 5 Average starch surface areas obtained from SEM images of ginger cubes dried by different methods

that the Midilli et al. model is the most apt for describing the changes in moisture ratio during the drying of ginger cubes using the EHD and EHD-hot air methods, as indicated by the statistical parameters. For the EHD method, the R^2 values ranged between 0.9996 and 0.9999, *RMSE* between 0.0017 and 0.0061, and χ^2 between 0.0273×10^{-4} and 0.3719×10^{-4}. In the case of the EHD-hot air combined method, R^2 values varied from 0.9996 to 0.9999, *RMSE* from 0.0024 to 0.0060, and χ^2 from 0.0615×10^{-4} to 0.3640×10^{-4}. For hot air applications at 50 and 55 °C, the Wang and Singh model yielded an R^2 value of 0.9999 for both scenarios, with *RMSE* and χ^2 values ranging between 0.0025 and 0.0031, and 0.0609×10^{-4} and 0.0947×10^{-4}, respectively. This model demonstrated the best fit to the experimental drying data for hot air. In Fig. 2, we present the experimental and predicted moisture ratio (*MR*) plotted against drying time, showcasing

close alignment between the two curves. These results parallel those of previous studies, with the Midilli et al. model found to best explain drying characteristics in mango ginger by Krishna Murthy and Manohar [32], in ginger by Loha et al. [33], and in onion and ginger by Khan et al. [34]. Furthermore, in line with our findings, the Wang and Singh model was identified as the best-fit model for experimental drying data in the studies conducted by Doymaz [35] and Sekhar et al. [36].

3.3 Effective diffusion coefficient (D_{eff})

Figure 3 displays the effective diffusion coefficient (D_{eff}) values of ginger cube slices under different drying methods. The D_{eff} values ranged between 1.733 and 6.566×10^{-8} m^2/s. These values fall within the typical range of 10^{-12} to 10^{-8}
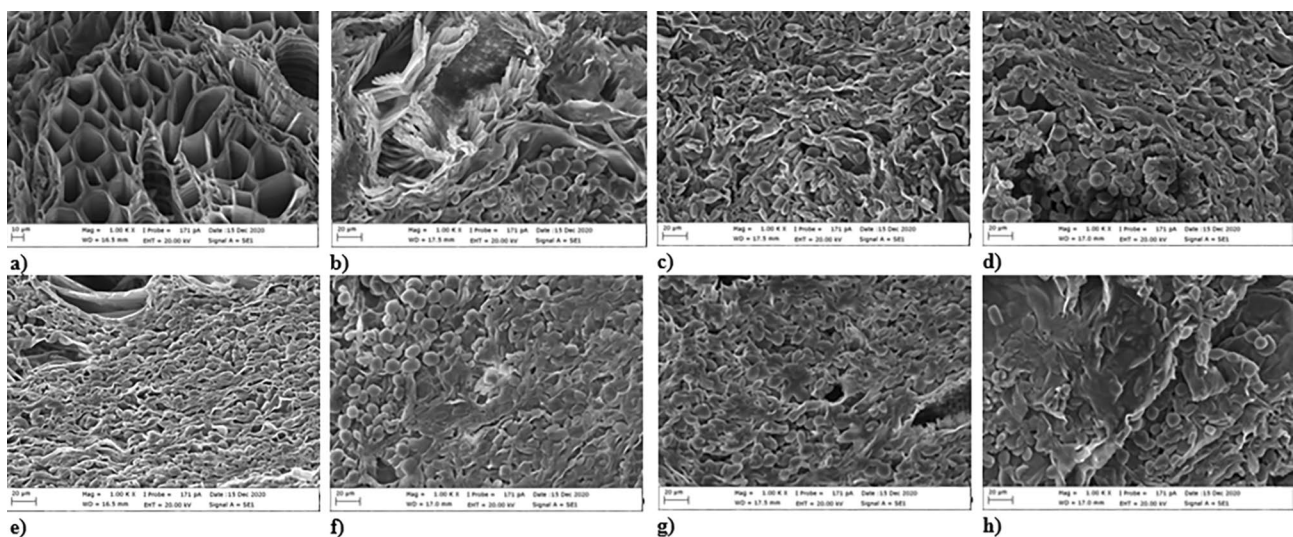

Fig. 4 Scanning electron microscope images of ginger cubes dried under different drying conditions: **a** 20 kV, **b** 30 kV, **c** 50 °C, **d** 55 °C, **e** 20 kV-50 °C, **f** 20 kV-55 °C, **g** 30 kV-50 °C, **h** 30 kV-55 °C

m^2/s for biological materials [37]. The highest value was obtained with 30 kV-55 °C application, while the lowest value was found with 20 kV application. As anticipated, in hot air applications, the effective moisture diffusion coefficient increased from 2.299×10^{-8} to 2.660×10^{-8} as the temperature increased from 50 °C to 55 °C [37]. The addition of EHD to hot air applications further increased the diffusion coefficient. The effective diffusion coefficient in 50 °C applications increased 2.31 times with the addition of 20 kV and 2.52 times with the addition of 30 kV. In EHD applications, the effective diffusion coefficient increased with the rise from 20 to 30 kV. In line with the findings of this study, Xiao and Ding [38] reported in their study of EHD drying of shiitake mushrooms that a higher voltage produced a stronger ionic wind, increased the water evaporation rate, and consequently resulted in a higher D$_{eff}$ value. Therefore, it is concluded that the EHD process can effectively improve the D$_{eff}$ value in the drying of ginger product.

3.4 Color analysis of ginger cubes

The color of a product serves as a critical parameter that reflects its overall characteristics and significantly influences consumer perceptions, either positively or negatively. Heat treatments applied to products can potentially result in the degradation of color pigments within their structure [39]. Table 4 presents the color values for both fresh ginger and ginger samples dried using various methods, including EHD, hot air, and EHD-hot air combinations. The color values for fresh products were determined as $L^* = 74.984 \pm 0.321$, $a^* = -3.244 \pm 0.027$, and $b^* = 40.478 \pm 0.089$. The drying methods had a significant impact on these color values, leading to an increase in a^* values while causing decreases in L^*, b^*, Chroma (C), and Hue angle ($\alpha°$) values [40]. Elevating both temperature and kV values within each method resulted in decreased L^* values. The treatment at 20 kV-50 °C yielded the L^* value closest to that of the fresh product, while the lowest L^* value was recorded for the 55 °C hot air treatment. In the hot air method, a^* values increased as temperature decreased [41]. Similarly, the EHD method showed an increase in a^* values with higher kV values. In the EHD-hot air combination method, a decline in b^* values was observed as temperature values increased within the same kV applications. This reduction in b^* values, indicating a loss of yellow color, may be attributed to non-enzymatic browning (Maillard) reactions, the breakdown of carotenoid pigments, and the formation of brown pigments [42]. Chroma (C) denotes color saturation, with higher values signifying vivid colors and lower values representing dull colors. The freshest product exhibited the highest C value, while the lowest values were observed in the 20 kV-55 °C and 20 kV treatments. C values decreased with increasing

temperature in the hot air method and with decreasing kV values in the EHD method. Hue angle ($\alpha°$) values ranged from 94.539 ± 0.046 (fresh) to 82.917 ± 0.047 (30 kV). The $\alpha°$ value closest to that of the fresh product was obtained with products subjected to the 55 °C hot air method. The total color difference (ΔE) value serves as a parameter indicating the distinction between the fresh and dried products, with lower ΔE values being preferred by consumers [43]. The lowest ΔE value was observed in the 20 kV-50 °C treatment. An increase in ΔE was noticed with increasing temperature in the EHD-hot air combined and hot air methods. In the EHD-only method, ΔE values did not exhibit significant changes with varying kV values. This finding contrasts with the results of Dinani et al. [7], who observed an increase in ΔE values as kV values were raised (from 17 and 19 kV to 21 kV) in their study on mushroom drying. This difference could be attributed to various experimental conditions, including temperature, humidity, the nature of the biological material, and the specific voltage values employed for EHD. Nevertheless, in the same study, the decrease in L^* values and the increase in a^* values with rising kV values demonstrated consistency with the outcomes of our research.

3.5 Microstructure of dried ginger cubes

Figure 4 provides a glimpse into the cross-sectional microstructures of ginger samples subjected to drying through different methods, including EHD, EHD-hot air, and hot air. An et al. [5] detected starch grains in fresh ginger tissue and observed a prominent parenchyma wall in fresh tissue, indicating that there was no cell breakage. They determined that breaks occurred in the cell wall with the effect of drying, and starch grains were distributed all over the tissue after drying. In this study, starch grains whose cell walls were broken with the effect of drying underwent gelatinization with different drying methods, resulting in a difference in surface area. Figure 5 shows the results of the measurements of the average surface areas of starch grains affected by varying voltage and temperature values of ginger samples dried by different methods.

In the EHD method, ginger samples dried with 20 kV exhibited a uniform honeycomb network structure in their microstructure. However, increasing the kV value led to the closure of pores and the development of burns in the microstructure. Although the skeletal structure was intact, the lowest value of starch surface area was found in the samples obtained from the 20 kV application. The starch surface area of the 30 kV treated products was higher than that of the 20 kV treated samples. Among the various EHD-hot air combination methods, those dried at 20 kV-50 °C managed to retain their skeletal structure better than the others. In contrast, products dried with the

30 kV-55 °C application showed the complete disappearance of their skeletal structure, with most starch granules becoming gelatinized. The surface area of starch samples that remained ungelatinized at high temperature and high voltage value was found to be higher than the products treated with low voltage value and temperature. The microstructure of products dried at 55 °C using the hot air method suffered severe damage compared to those dried at 50 °C. Notably, the starch granules in ginger samples dried at 50 °C with hot air exhibited a lower degree of gelatinization compared to samples dried at 55 °C. As in the EHD-hot air combination method, the starch surface area of ginger samples dried at high temperature was higher than the products dried at low temperature in the hot air method. In fact, the starch in samples dried at 55 °C was not fully dissolved, in line with the findings of Huang et al. [44]. These observations highlight the detrimental effects of high temperatures on the microstructure of the product, a phenomenon also noted by Wang et al. [45] in their study on ginger drying.

4 Conclusions

In this study, ginger samples underwent drying processes using EHD, hot air, and EHD-hot air methods, with a constant air velocity of 1.5 m/s. The primary objectives of this investigation were to evaluate various aspects, including drying time, mathematical modeling, color, and microstructure properties of the resulting dried ginger cubes. Notably, the EHD-hot air combination method demonstrated a shorter drying time compared to the other techniques employed. Modeling studies, supported by statistical results, identified the Midilli et al. and Wang and Singh models as particularly well-suited for elucidating the drying mechanisms of ginger cubes. In all drying conditions, an increase in temperature and voltage values led to an increase in the diffusion coefficient. Furthermore, a decrease in b* values was observed with reduced kV in the EHD method and increased temperature values in the hot air method. As temperature and voltage values increased, there was a significant reduction in starch grains, leading to alterations in their structure and distribution within the product. Additionally, starch surface areas were found to be larger in the samples treated at higher temperature and voltage values than in the samples treated at lower volt values. This study on the drying behavior of ginger samples using EHD, EHD-hot air, and hot air methods provides valuable insights that can inform future research in the field of drying technology. Additionally, our findings suggest the potential for integrating EHD technology with hot air systems in the development of efficient drying devices.

Declarations

References

1. Li H, Liu Y, Luo D, Ma Y, Zhang J, Li M, Yao L, Shi X, Liu X, Yan K (2019). Complement Ther Med. https://doi.org/10.1016/j.ctim.2019.06.002
2. Kate AE, Sutar PP (2018). Innov Food Sci Emerg Tech. https://doi.org/10.1016/j.ifset.2018.05.021
3. Jung MY, Lee MK, Park HJ, Oh EB, Shin JY, Park JS, Young SY, Oh JH, Choi DD (2018). Food Sci Biotechnol. https://doi.org/10.1007/s10068-017-0301-1
4. Lin X, Xu JL, Sun DW (2020). Food Chem. https://doi.org/10.1016/j.foodchem.2020.127407
5. An K, Zhao D, Wang Z, Wu J, Xu Y, Xiao G (2016). Food Chem. https://doi.org/10.1016/j.foodchem.2015.11.033
6. Esehaghbeygi A, Basiry M (2011). J Food Eng. https://doi.org/10.1016/j.jfoodeng.2011.01.032
7. Dinani ST, Hamdami N, Shahedi M, Havet M (2015) D. Food Bioprod Process. https://doi.org/10.1016/j.fbp.2015.04.001
8. Dinani ST, Hamdami N, Shahedi M, Havet M (2015). Food Bioprod Process. https://doi.org/10.1016/j.fbp.2014.08.004
9. Martynenko A, Zheng W (2016). J Food Eng. https://doi.org/10.1016/j.jfoodeng.2015.07.043
10. Caliskan G, Dirim SN (2017). Heat Mass Transf. https://doi.org/10.1007/s00231-017-1967-x
11. Pirnazari K, Esehaghbeygi A, Sadeghi M (2016). Int J Food Eng. https://doi.org/10.1515/ijfe-2015-0005
12. Sacilik K, Unal G (2005). Biosyst Eng. https://doi.org/10.1016/j.biosystemseng.2005.06.006
13. Amiri Chayjan R, Shadidi B (2014). J Food Process Preserv. https://doi.org/10.1111/j.1745-4549.2012.00766.x
14. Bhattacharya M, Srivastav PP, Mishra HN (2015). J Food Sci Technol. https://doi.org/10.1007/s13197-013-1209-2
15. Ergün K, Çalışkan G, Dirim SN (2016). Heat Mass Transf. https://doi.org/10.1007/s00231-016-1773-x
16. Belghith A, Azzouz S, ElCafsi A (2016). Heat Mass Transf. https://doi.org/10.1007/s00231-015-1560-0
17. Perea-Flores MJ, Garibay-Febles V, Chanona-Perez JJ, Calderon-Dominguez G, Mendez-Mendez JV, Palacios-González E, Gutiérrez-López GF (2012). Ind Crop Prod. https://doi.org/10.1016/j.indcrop.2012.01.008
18. Taşkın O, İzli G, İzli N (2018). J Agric Sci. https://doi.org/10.15832/ankutbd.456654
19. Midilli A, Kucuk H, Yapar Z (2002). Dry Technol. https://doi.org/10.1081/DRT-120005864
20. Won YC, Min SC, Lee DU (2015). Dry Technol. https://doi.org/10.1080/07373937.2014.999371
21. Uddin Z, Suppakul P, Boonsupthip W (2016). Dry Technol. https://doi.org/10.1080/07373937.2015.1119840
22. Crank J (1979) The Mathematics of Diffusion. Oxford University Press, New York

23 Majumder P, Sinha A, Mishra L, Gupta R (2020) In Advances in Mechanical Engineering: Select Proceedings of ICRIDME 2018 (pp. 729–740). Springer Singapore. https://doi.org/10.1007/978-981-15-0124-1_66.

24. Wang J, Law CL, Nema PK, Zhao JH, Liu ZL, Deng LZ, Gao ZJ, Xiao HW (2018). J Food Eng. https://doi.org/10.1016/j.jfoodeng.2018.01.002

25. Seerangurayar T, Al-Ismaili AM, Jeewantha LJ, Al-Habsi NA (2019). Food Bioprod Process. https://doi.org/10.1016/j.fbp.2019.03.012

26. Deng LZ, Yang XH, Mujumdar AS, Zhao JH, Wang D, Zhang Q, Wang J, Gao ZJ, Xiao HW (2018). Dry Technol. https://doi.org/10.1080/07373937.2017.1361439

27. Thilagashanthi T, Gunasekaran K, Satyanarayanan KS (2021). J Clean Prod. https://doi.org/10.1016/j.jclepro.2021.129217

28. Pirone BN, De Michelis A, Salvatori DM (2014). Food Bioproc Technol. https://doi.org/10.1007/s11947-013-1238-x

29. Li FD, Li LT, Sun JF, Tatsumi E (2005). Dry Technol. https://doi.org/10.1081/DRT-200054133

30. Taghian Dinani S, Havet M, Hamdami N, Shahedi M (2014). Dry Technol. https://doi.org/10.1080/07373937.2013.851086

31. Sadeghi M, Mirzabeigi Kesbi O, Mireei SA (2013). J Sci Food Agric. https://doi.org/10.1002/jsfa.5786

32 Krishna Murthy TP, Manohar B. (2012) Int J Food Sci Technol. https://doi.org/10.1111/j.1365-2621.2012.02963.x

33. Loha C, Das R, Choudhury B, Chatterjee PK (2012). J Food Process Technol. https://doi.org/10.4172/2157-7110.1000160

34. Khan MKI, Maan AA, Aadil RM, Nazir A, Butt MS, Rashid MI, Afzal MI (2020). Food Sci Biotechnol. https://doi.org/10.1007/s10068-019-00695-5

35 Doymaz İ (2011) J Food Process. Preserv. https://doi.org/10.1111/j.1745-4549.2011.00557.x

36. Sekhar YR, Pandey AK, Mahbubul IM, Avinash GRS, Venkat V, Pochont NR (2021). Sol Energy. https://doi.org/10.1016/j.solener.2021.08.011

37. Doymaz İ (2017). Heat Mass Transf. https://doi.org/10.1007/s00231-016-1791-8

38. Xiao A, Ding C (2022). Foods. https://doi.org/10.3390/foods11091303

39. Saxena A, Maity T, Raju PS, Bawa AS (2012). Food Bioproc Technol. https://doi.org/10.1007/s11947-010-0409-2

40. Izli N, Polat A (2019). Food Sci Technol. https://doi.org/10.1590/fst.04518

41. Aral S, Beşe AV (2016). Food Chem. https://doi.org/10.1016/j.foodchem.2016.04.128

42. Demiray E, Tulek Y (2015). J Food Process Preserv. https://doi.org/10.1111/jfpp.12290

43. Bai JW, Sun DW, Xiao HW, Mujumdar AS, Gao ZJ (2013). Innov Food Sci Emerg Technol. https://doi.org/10.1016/j.ifset.2013.08.011

44. Huang TC, Chung CC, Wang HY, Law CL, Chen HH (2011). Dry Technol. https://doi.org/10.1080/07373937.2011.589554

45. Wang J, Bai TY, Wang D, Fang XM, Xue LY, Zheng ZA, Gao Z.J, Xiao HW (2019). Dry Technol. https://doi.org/10.1080/07373937.2017.1423325